



# Obtaining archaeointensity data from British Neolithic pottery: A feasibility study

Megan L. Allington<sup>a,\*</sup>, Catherine M. Batt<sup>b</sup>, Mimi J. Hill<sup>c</sup>, Andreas Nilsson<sup>a</sup>, Andrew J. Biggin<sup>c</sup>, Nick Card<sup>d</sup>

<sup>a</sup> Department of Geology, Lund University, Lund, Sweden

<sup>b</sup> School of Archaeological and Forensic Sciences, University of Bradford, Bradford BD7 1DP, UK

<sup>c</sup> Geomagnetism Laboratory, School of Environmental Sciences, University of Liverpool, Liverpool L69 7ZE, UK

<sup>d</sup> University of Highlands and Islands Archaeology Institute, Orkney College, East Rd, Kirkwall KW15 1LX, UK

## ARTICLE INFO

### Keywords:

Archaeointensity

Neolithic

Grooved ware

Geomagnetic secular variation

## ABSTRACT

There is a significant lack of geomagnetic field strength (archaeointensity) measurements for many archaeological time periods in the United Kingdom (UK). This not only makes past geomagnetic secular variation difficult to model but also limits the development of archaeointensity dating. This paper presents the first archaeointensity study on UK Neolithic material. In this study, twenty-five sherds of Neolithic Grooved Ware pottery from the Ness of Brodgar, Orkney, UK, some with direct radiocarbon dates, were subjected to a full archaeomagnetic investigation with the aim of increasing the amount of archaeointensity data for the UK. Both thermal Thellier and microwave palaeointensity experiments were used to determine which technique would be most suitable for British Neolithic pottery. Three successful archaeointensity results between 35 and 40  $\mu$ T were obtained using thermal Thellier method, which is consistent with the limited data available within a 15° radius and geomagnetic field model predictions from the same time. We separated the results into four different types with an intention of explaining the behaviours that determine the likelihood of achieving an acceptable archaeointensity estimate. The feasibility of obtaining geomagnetic field strength information during the UK Neolithic from ceramics has been demonstrated and the results provide a solid basis for improving our knowledge of geomagnetic secular variation during archaeological time in Britain.

## 1. Introduction

The fundamental principle of archaeomagnetism is that heated archaeological materials acquire a magnetisation that is distinctive to that time period (and location) and is retained over archaeological timescales. This magnetisation can be dated by comparison with a previously determined record of the variation of the geomagnetic field over time for that location. The dating comparison can be made on the basis of the direction of the magnetic field (declination and inclination) or the intensity (strength), or by a combination of both.

There have been direct measurements of the geomagnetic field in the UK for approximately the last 400 years (Malin et al., 1981; Jonkers et al., 2003) but prior to that, secular variation is determined from magnetic measurements on materials with an independent date (e.g. Clark et al., 1988). The first secular variation curve for the UK was developed by Aitken et al. (1963), however this only used declination

and inclination, and the subsequent focus of archaeomagnetic dating in the UK has continued to be on directions (e.g. Clark et al., 1988; Zanani et al., 2007; Batt et al., 2017). Consequently, there is a dearth of past field strength (archaeointensity) measurements for the UK and those that exist are from pilot studies that have been undertaken on single features (e.g. Casas et al., 2005). All available archaeomagnetic data, including archaeointensity measurements, for the UK are compiled and modelled in Batt et al. (2017) in the form of geomagnetic model ARCHUK.1.

Archaeointensity studies are more numerous in other countries in Europe, such as France (e.g. Genevey et al., 2013; Hervé et al., 2013) and Bulgaria (Kovacheva, 1997; Kovacheva et al., 2009). Archaeointensity research is also abundant in the Near East (e.g. Ben-Yosef et al., 2009; Shaar et al., 2011). Few archaeomagnetic datasets reach as far back as the British Neolithic, which is defined as 4000BCE–2000BCE (Forum on Information Standards in Heritage, 2016) therefore studies of material

\* Corresponding author.

E-mail address: [megan.allington@geol.lu.se](mailto:megan.allington@geol.lu.se) (M.L. Allington).

<https://doi.org/10.1016/j.jasrep.2021.102895>

Received 13 October 2020; Received in revised form 15 February 2021; Accepted 20 February 2021

Available online 11 March 2021

2352-409X/© 2021 The Authors. Published by Elsevier Ltd. This is an open access article under the CC BY license (<http://creativecommons.org/licenses/by/4.0/>).

from this period are important both for establishing reference curves for archaeomagnetic dating and more generally for understanding the past behaviour of the geomagnetic field.

Although archaeointensity dating is less developed than its archaeodirectional counterpart, it has still been able to produce new insights into the archaeological record. For example, in [Stillinger et al. \(2015\)](#), archaeointensity estimates taken from ceramics excavated from the same context at Tell Mozan, Syria have identified an intrusive sherd due to a discrepancy in archaeointensity values. Pottery is an ideal material for dating by archaeointensity (once reference curves are established) as there is a plethora of pottery surviving within the archaeological record. Pottery cannot be dated using archaeodirections since the orientation of the pot during the initial firing is unknown. Accordingly, the development of archaeomagnetic dating by intensity could have far-reaching implications in terms of understanding archaeological chronologies.

In this paper, we present the results of an archaeomagnetic investigation of Orcadian Neolithic pottery. Firstly, the study aims to investigate whether Neolithic pottery of the type exemplified by the Ness of Brodgar retains a measurable record of the past magnetic field and secondly if this record is comparable to data from elsewhere in Europe for that period. This publication presents the first results for such an investigation on UK Neolithic material. Due to the sparsity of archaeointensity data in both higher latitudes and for the Neolithic, the Orcadian Neolithic is a high priority when looking for possible new sites for archaeointensity investigations.

High failure rates in archaeointensity experiments are common, especially from poorly fired material. Possible reasons for failure include alteration of the magnetic minerals during the experiment and multi-

domain grain behaviour (the theory behind the experiments are for single domain magnetic grains). A full rock magnetic study was carried out in order to characterise the magnetic mineralogy of the sample set and to determine their suitability for archaeointensity study. Archaeointensity studies could be far more productive if the method of measurement was optimised. In an attempt to maximise the success of the experiments this project made measurements using two different demagnetisation methods, both thermal ([Thellier and Thellier, 1959](#)) and microwave (MWS) ([Walton et al., 1993; Hill and Shaw, 1999](#)).

## 2. Archaeological context

The Ness of Brodgar ([Fig. 1](#)), sits within the ‘Heart of Neolithic Orkney’ World Heritage Site, on Mainland Orkney, Scotland, UK (58.9970°N, 3.2149°W). The site was discovered by geophysical survey in 2002 and eight test trenches were opened in the summer of 2004 ([Card, 2012](#)). Since then there have been annual, large-scale area excavations, managed by Orkney Research Centre for Archaeology (ORCA) and the Ness of Brodgar Trust. This has revealed a deeply stratified, multi-phase Neolithic complex. In the main phases presently under investigation the site was dominated by many huge, freestanding buildings partly enclosed by massive stone walls. The size, quality and architecture of these buildings, combined with rich assemblages of artefacts, evidence of tiled roofs, coloured walls and pottery, exotic material from across Britain, and over 900 examples of decorated stone imply that this was not a domestic settlement. During its main phases it was a place of coming together for people from across Orkney and beyond, and where they took part in exchange, feasting and conspicuous



**Fig. 1.** A. Map showing the location of the Ness of Brodgar, Mainland Orkney, Scotland. [Fig. 1B](#) and [C](#). Aerial photos of the site. Map: ORCA. Aerial photos: Scott Pike.

consumption (Card, 2018).

The Ness of Brodgar was selected as the focus of this study due to the longevity of activity, large pottery assemblage and numerous associated radiocarbon dates interpreted within a Bayesian statistical framework (Card et al., 2017). Preliminary radiocarbon dates suggested continuous habitation between 3200BCE and 2200BCE, after which the site was decommissioned and abandoned. However, a new formal chronological model, undertaken with further radiocarbon dates and recent fieldwork results (Card et al., 2017), has suggested punctuated and intermittent activity over a more extended timeframe.

The most common Orcadian Neolithic pottery types are Unstan Ware and Grooved Ware. Grooved Ware has been found at over 50 sites in Neolithic Scotland alone (Cowie and MacSween, 1999) and is the main type of pottery excavated at the Ness of Brodgar. Grooved Ware pottery is typically friable and fired in open fires. The exact details of how the pottery is cooled at the end of the firing process is unknown however this is expected to be on the scale of hours as opposed to minutes or days. Examples of the Grooved Ware used in these experiments are shown in Fig. 2.

### 3. Archaeomagnetic investigation

#### 3.1. Sample selection

Twenty-five pottery samples were selected for the various experiments from the vast assemblage available from the Ness of Brodgar excavations. The selection criteria were that the samples should be from well-dated contexts and cover a variety of deposits and different structures at the Ness of Brodgar. All the samples were excavated between the field seasons of 2010 and 2015. Structures 1, 8, 10, 12 and 14 are represented in the sample set. Six small find numbers of this sample set have direct radiocarbon dates attached to them (Card et al., 2017), taken from carbonised residue from the sherds (see Supplementary Table S1) as part of the Times of Their Lives project (Whittle, 2017). The radiocarbon dates were calibrated using IntCal13 (Reimer et al., 2013). For eleven samples the radiocarbon date is from a different sample taken from the same context and thus assumed to be of similar age. The remaining 8 samples came from contexts within structures where there are too few radiocarbon dates so that the age assigned is taken as a likely age range from the primary build of the structure to the last usage (Card pers. comm). See Supplementary Table S1.

#### 3.2. Magnetic mineralogy investigation

In order to investigate the magnetic mineralogy, the samples were

analysed using a Variable Field Translation Balance (VFTB) at the Geomagnetism Laboratory, University of Liverpool. For each of the 25 pottery sherds, a fragment of between 120 and 200 mg was ground to a fine powder in a pestle and mortar. The powder was then transferred into a glass sample holder and sealed with quartz wool. The samples were then exposed to a series of experiments with temperatures up to 700 °C and an ambient field up to 800mT in order to obtain isothermal remanent (IRM) acquisition curves, backfield coercivity measurements, hysteresis loops and thermomagnetic curves. Results were analysed in the software RockMagAnalyser1.0 (Leonhardt, 2006) and all are given in Supplementary Table S1 with representative results shown in Figs. 3 and 4.

Similar behaviour is found for all of the Ness of Brodgar sherds analysed. IRM curves indicate the magnetization of all samples saturates by 350mT; an example is shown in Fig. 3A. Thus, there is no evidence for any high coercivity mineral such as haematite. Coercivity ranges from 20mT to 60mT (an example hysteresis loop is shown in Fig. 3B). All the hysteresis loops are pot-bellied, indicating that the pottery has multiple coercivity fractions.

The hysteresis ratios of saturation of remanent magnetisation to saturation magnetisation  $M_{rs}/M_s$  versus coercivity of remanence to coercivity  $B_{cr}/B_c$  are plotted on a Day plot in Fig. 3C (Day et al., 1977). There is a spread of values lying on or above the Dunlop (2002) mixing curves with  $M_{rs}/M_s$  ranging from 0.13 to 0.33 suggesting magnetic grain sizes fall in the so called pseudo-single domain region. Whilst no samples plot within the multi domain grain region (indicating potential unsuitability for archaeointensity experiments) the limitations of the Day plot are recognised (Roberts et al., 2018).

Curie Temperatures were determined by taking the second derivative of the heating-cooling curves within the RockMagAnalyser1.0 software (Leonhardt, 2006). The dominant Curie temperature ranges from 515 °C to 614 °C with 16% having a Curie Temperature above that of magnetite 585 °C. Sixty percent of the samples have reversible heating-cooling curves (Fig. 4A). The distinctive kinked shape observed in the remaining forty percent of the thermomagnetic curves happens during heating, but does not reappear as the sample is cooled down (Fig. 4B).

In order to investigate whether the inflection seen in some of the Curie curves is indicative of a lower Curie temperature phase or if it is the signature of alteration at this temperature, two selected sister samples underwent further experiments. Repeated heating/cooling cycles were run at successively higher temperatures (from room temperature up to maximum of 700 °C) in order to see at what temperature, the heating and cooling curves differed (Fig. 4C). The heating and cooling curves are identical until 300 °C, which indicates that the alteration

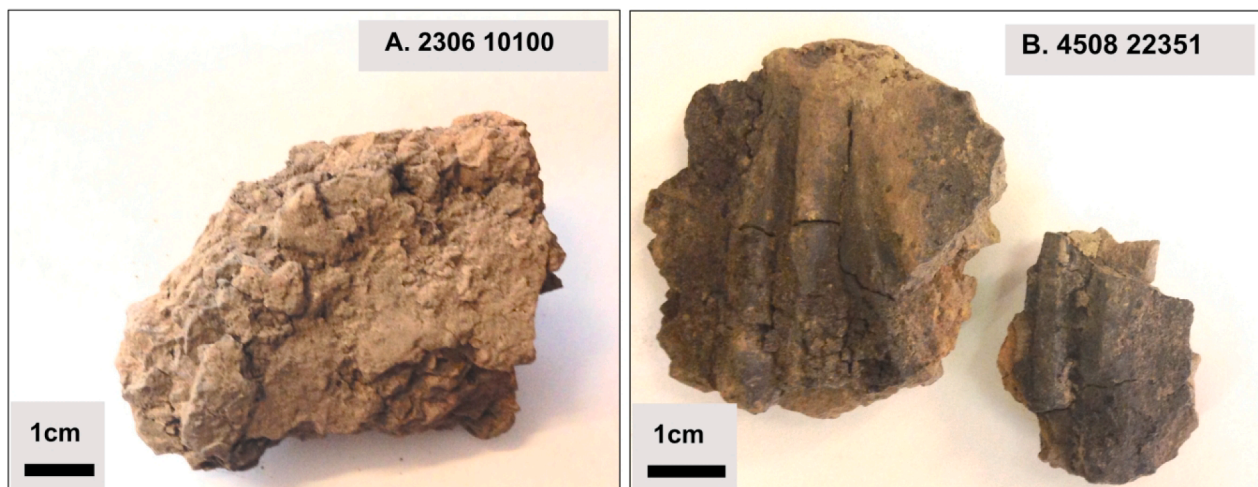
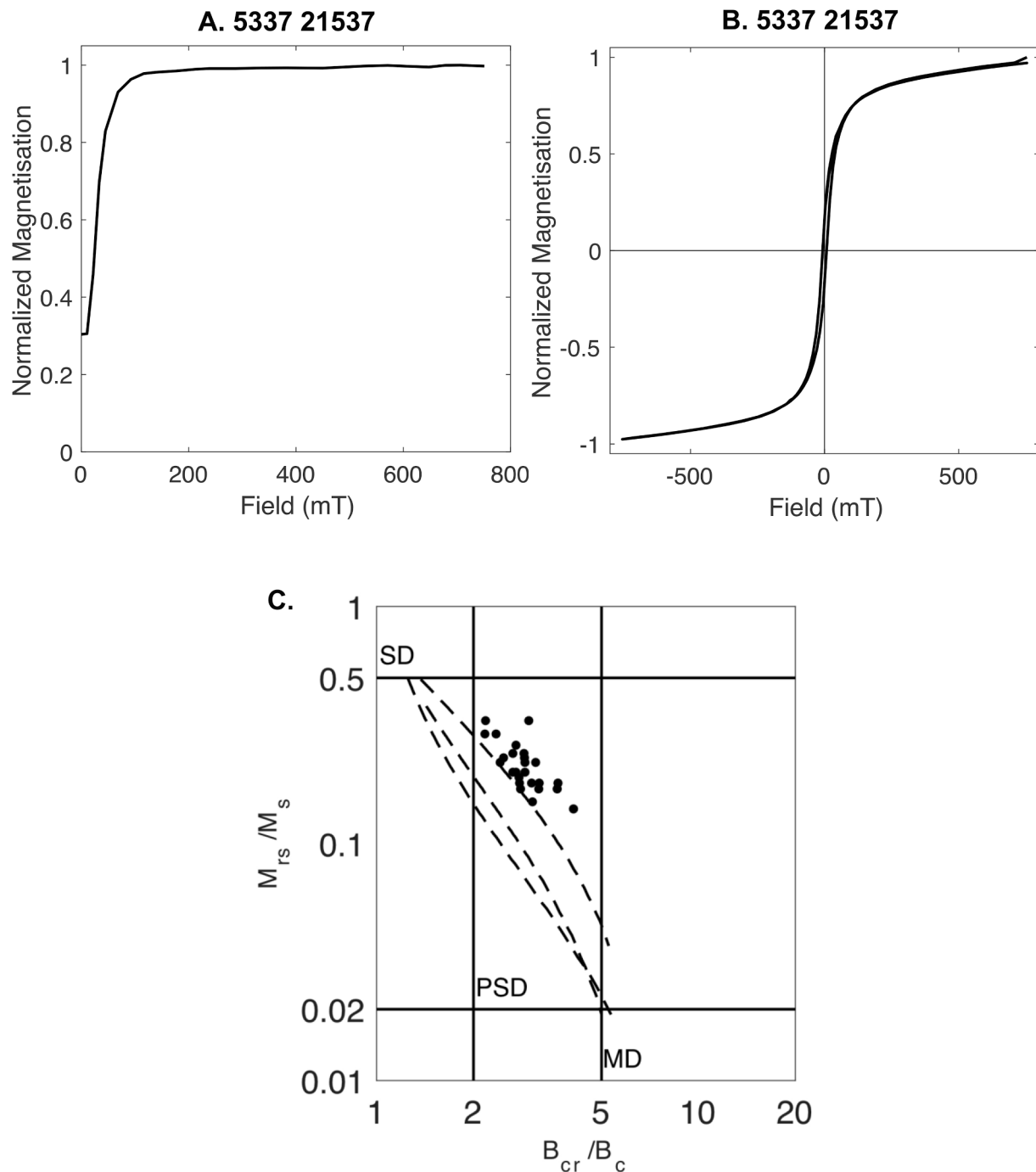


Fig. 2. Photographs of a selection of the Grooved Ware samples used in this study.





**Fig. 3.** A. IRM plot, and Fig. 3B. hysteresis plot for a representative sample 5337 21957. Fig. 3C. Day plot (Day et al., 1977) of saturation of remanent magnetisation to saturation magnetisation ( $M_{rs}/M_s$ ) versus coercivity of remanence to coercivity ( $B_{cr}/B_c$ ) for all 25 of the Ness of Brodgar samples. SD is single domain, PSD is pseudo-single domain and MD is multi-domain. The dashed lines are SD and MD mixing curves from Dunlop (2002).

occurs from there and it continues in the subsequent heating steps in a similar manner with the cooling curve above the heating curve until the 600 °C heating step. This suggests that the kink seen in the curve is due to the creation of a higher magnetisation phase between approximately 300 °C to 600 °C. The heating and cooling curves are identical for the 600 °C step but then further alteration occurs after heating to 700 °C with the cooling curve much below the heating curve indicating alteration to a lower magnetisation phase.

Overall, the results are consistent with a magnetic mineralogy of predominantly Ti-poor titanomagnetite with no evidence for the addition of any higher coercivity mineral. This mineralogy is suitable for

archaeointensity analysis. As some samples exhibit a Curie Temperature above that of magnetite, it could suggest the presence of maghaemite which is also suitable mineralogy assuming it was formed prior to the clay formation. At lower temperatures (under 300 °C), there is a transformation to a higher magnetisation mineral which if remanence carrying will cause an archaeointensity experiment to fail. Common transformations for poorly fired pottery (as is the nature of the Ness of Brodgar sherds) include titanium-poor titanomagnetite to magnetite at around 200 °C (Dunlop and Özdemir, 1997) and oxidation of magnetite into maghaemite (Atkinson and King, 2005) or the inversion of titanomaghaemite to titanomagnetite. There is evidence for alteration at high

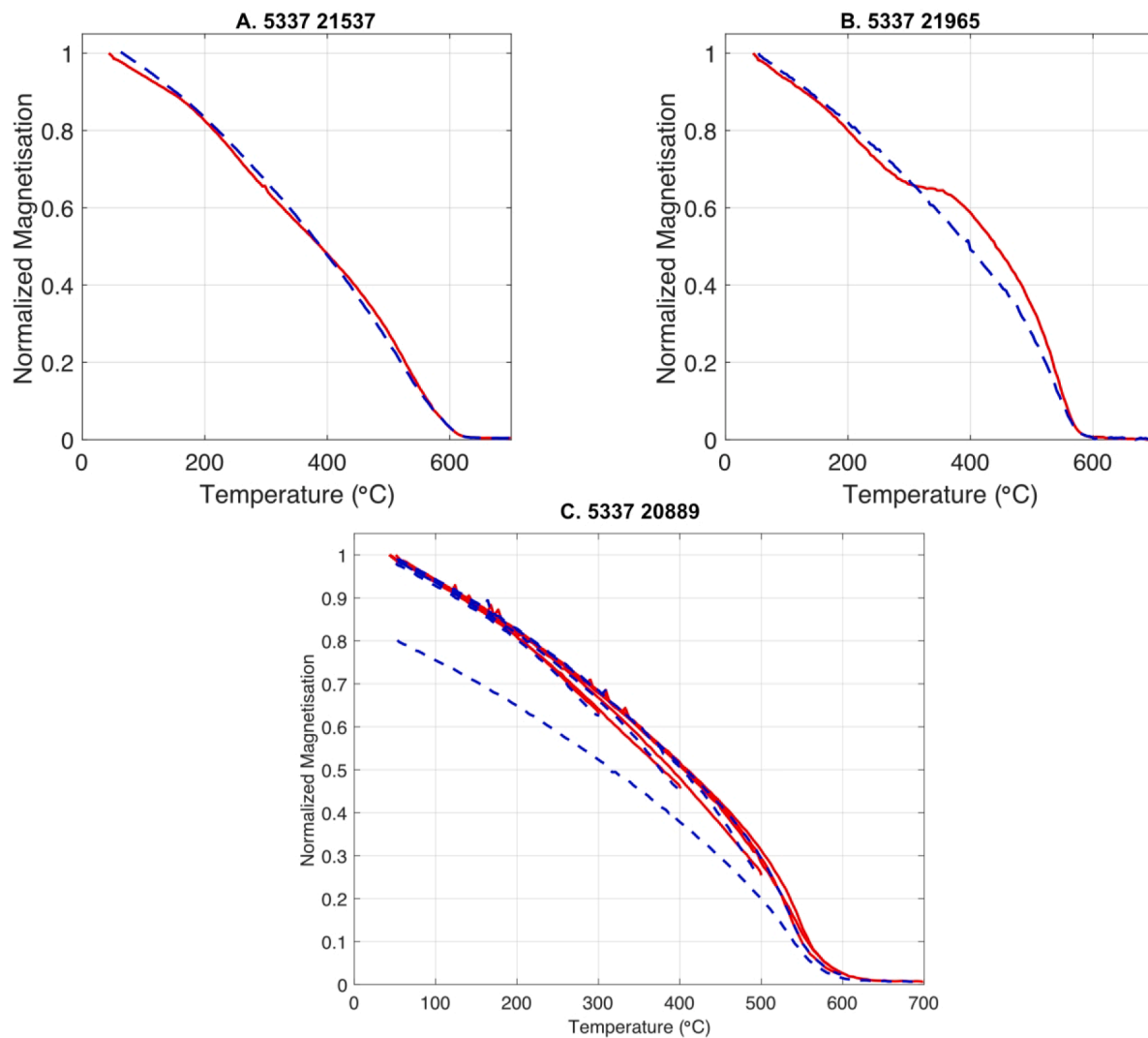


**Fig. 4.** A. Thermomagnetic plot for sample 5337 21957. Fig. 4B. thermomagnetic plot for sample 5337 21965. Sample 5337 21,957 shows minimal alteration whilst sample 5337 21,965 shows that there is a change to a weaker magnetised phase during heating. Red lines: heating. Blue lines: cooling. Fig. 4C. Cyclic temperature VFTB experiment for sample 5337 20,889 to further map the sample alteration. The alteration is most significant after heating to 700 °C. Red solid lines: heating. Blue dashed lines: cooling. (For interpretation of the references to colour in this figure legend, the reader is referred to the web version of this article.)

temperature (above 600 °C) for an additional alteration to a less magnetic phase such as oxidation of magnetite to haematite.

### 3.3. Archaeointensity experiments

Archaeointensity experiments were carried out using two different methods, thermal and microwave at the Geomagnetism Laboratory, University of Liverpool. There have been many studies which show that archaeointensity results obtained through thermal and microwave methods are comparable (e.g. Hill et al., 2002; Stark et al., 2010) so the results collected are expected to be analogous. The first archaeointensity experiments were undertaken on the microwave system (MWS). It consists of a 14 GHz microwave de/remagnetiser combined with a low temperature Tristan SQUID magnetometer. For these experiments, the sherds were drilled into cores of diameter 5 mm and 2 mm in length. The pottery sherds were very delicate and crumbled under the pressure from the drill and were not easily consolidated, so only 5 samples were obtained. The thermal archaeointensity experiments were undertaken using a Magnetic Measurements Thermal Demagnetiser and an AGICO JR6 magnetometer. For these experiments, 17 of the sherds (ignoring the most friable samples but including 4 of the 5 that underwent MWS

experiments) were trimmed and inserted into glass tubes 12 mm in diameter. The sample was placed inside the tube and the ends sealed with quartz wool. To ensure that the wool stayed fixed, a solution of 70% sodium silicate and 30% water was pipetted over the ends of the tube.

The IZZI+ protocol (Yu et al., 2004) was used for both sets of experiments with a laboratory in-field step of 50  $\mu$ T aligned along the z axis of the glass tubes / cores. Anisotropy of remanence was monitored by comparing the direction of the laboratory induced remanence to the direction of the applied field, the so-called gamma factor (Biggin and Paterson, 2014; Paterson et al., 2014). Separate experiments to investigate the dependence of the remanence on cooling rate were not carried out. Archaeointensity results were deemed successful if they passed the selection criteria SELCRIT2 which is a combination of parameters to statistically assess and give cause to accept an archaeointensity result (Biggin et al., 2007; Paterson et al., 2014) and if anisotropy of remanence was deemed negligible.

No successful archaeointensity results were obtained for the 5 samples that were investigated with the MWS, due in part to technical issues. As previously mentioned the sherds were not suitable to be prepared in large numbers for the MWS due to their friable texture. This texture also caused problems with the vacuum attachment used to hold samples in

the MWS. The drill core should have a smooth surface in order to adhere securely but the pottery texture was too rough for proper adhesion, therefore samples often became unattached before the experiment's completion. The pottery also exhibited unusual behaviours during the microwave application. The MWS uses microwaves to impart energy into the magnetic minerals in the sample. To select the frequency that will allow the most effective energy absorption the resonance frequency is determined. This resonance frequency is dependent on such things as the sample material, size, and position within the microwave cavity. In these experiments, the resonance frequency varied between each step of the experiment resulting in the sample under investigation not absorbing the same amount of energy for each pair of steps in the IZZI+ protocol.

The results were analysed using paleointensity.org, an open source application (Béguin et al., 2020). For the thermal experiments three samples out of seventeen produced archaeointensity results that passed the SELCRIT2 criteria (Biggin et al., 2007; Paterson et al., 2014), which corresponds to a success rate of 18%. The results are shown in Fig. 5 and the successful results are summarised in Table 1, alongside selection criteria from SELCRIT2. The successful archaeointensity estimates range from between 35  $\mu$ T and 40  $\mu$ T. Anisotropy was found to be minimal with the angle between the laboratory induced TRM direction and the direction of the applied inducing field (gamma factor) less than 4° for the three samples (also found in Table 1).

Eight out of the seventeen samples exhibited more complex magnetisation history with multiple components of magnetisation present or a significant overprint. The sister samples that underwent microwave experiments also showed the same demagnetisation behaviour. Other reasons for failure of the experiments were failed alteration (pTRM) checks, zig zagging and / or curved Arai plots indicating MD behaviour or a combination of all the above. Reasons for failure are indicated in Supplementary Table S1.

## 4. Discussion

### 4.1. Minimising undesirable behaviour in future experiments

This study is the first rock magnetic and archaeointensity study of Orcadian Neolithic pottery, the results of which we anticipate will lead to potential refinements and an increased success rate in similar studies in the future. Although it would be advisable to recommend less friable samples in future investigations, it is not always possible in archaeology. Some sites may not have ideal preservation conditions or provide only low fired pottery sherds, in these cases we argue that archaeointensity experiments still provide valuable information so the following recommended protocols are still relevant.

From the work undertaken here, we recommend that future investigations should primarily focus on thermal Thellier experiments to increase the likelihood of obtaining an accepted archaeointensity result. The friable nature of the pottery meant that sample preparation for the MWS was challenging and the issues with absorbed energy reproducibility during the experiment meant that the IZZI+ protocol was not feasible. Some form of consolidation (e.g. sodium silicate impregnation under vacuum) of the complete pottery sherds prior to any sub-sampling is recommended for both microwave and thermal methods. The MWS could demagnetise the samples and so further investigations could be worthwhile using a different experimental protocol (i.e. not IZZI+) or if the reason for the changing resonance frequency of the sample be ascertained. This behaviour is not found routinely for pottery and ceramics as there are many examples of successful studies (e.g. Stark et al., 2010; Calvo-Rathert et al., 2019). It is possible that the sample was not firmly held on via the vacuum so that it was in a slightly different position within the cavity each time, or it is possible the sample was altering in some way that changed the behaviour to microwave exposure.

In order to classify typical sample behaviours, with a hope to identify

behaviours that limit the likelihood of achieving an acceptable archaeointensity estimate we separated the magnetic mineral behaviours found into four types: all samples have been typed (see Supplementary Table S1). We begin with type 1: an accepted archaeointensity result, of which three were produced in this study (Fig. 5A, B and C).

Type 2 indicates that the sample experience some form of alteration when exposed to heating. This can be seen from the Curie Curves and also seen during an archaeointensity experiment as a failed pTRM check. An example is shown in Fig. 4B.

Type 3 is where a sample is affected by remanence contained within multi-domain grains. This is typically indicated by a zig zag behaviour on the Arai plot. If the magnetic mineralogy is dominated by MD grains this can be seen in the hysteresis parameters.

Type 4 samples have multiple components of magnetisation, or overprints. This is found from the orthogonal vector plots obtained during the archaeointensity experiment (see e.g. Fig. 5D). It indicates that the last heating of the sample did not fully remagnetise it and so was at a temperature lower than the highest blocking temperature. This is common in archaeological pottery as open fires provide uneven temperature gradients leading to not well-fired pottery.

There is some cross-over behaviour between types (Supplementary Table S1), especially between the different failed experiments, with some samples from the experiments exhibiting up to three different types of behaviour.

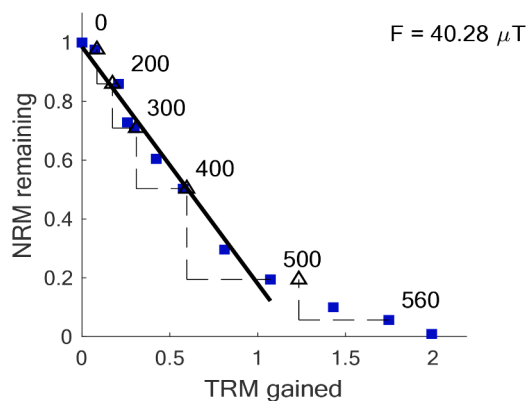
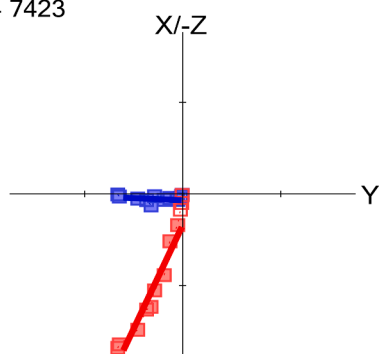
Thermochemical alteration of the samples upon heating has proven to be problematic in this study. Thermomagnetic curves and especially the detailed repeated heating to higher temperature cycles are useful to determine whether the samples are likely to alter on heating. Running experiments like these before an archaeointensity experiment would allow the selection of samples that have non-reversible thermomagnetic curves, hence increasing the chance of gaining type 1 results. However, it is noted that one accepted result (2114 7423) does show alteration in the heating-cooling Curie curve. However, during the archaeointensity experiment the pTRM checks do not fail in the section of the Arai plot where the archaeointensity estimate is derived and all SELCRIT2 criteria are satisfied. Therefore, relying solely upon rock magnetic analysis may be removing more samples than necessary.

From the hysteresis parameters no samples studied exhibit bulk multi-domain behaviour. It is common however for a material to contain a mix of both single- and multi-domain grains with the bulk indicative of a so-called pseudo single domain grain size. Some evidence of MD behaviour was seen within the archaeointensity experiments suggesting that for some samples MD behaviour could be a cause of failure but it was not as prevalent as alteration.

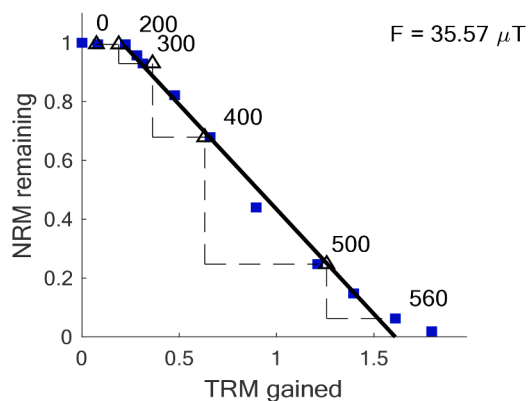
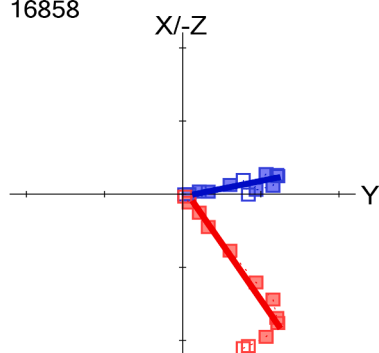
Not all behaviours can be identified from rock magnetic experiments alone. Type 4 can only be observed in a demagnetisation or archaeointensity experiment. For future investigations we recommend running pilot demagnetisation experiments as nearly half of our sample set showed overprints of some form. Demagnetisation experiments are much quicker to complete than intensity experiments.

Interesting information is contained within the overprints however and approaching further archaeointensity experiments with a multi-vectorial approach similar to Yu and Dunlop (2002) could allow a higher yield of archaeointensity results. The premise of multivectorial analysis is that a different archaeointensity result is obtained for each distinct overprint. This allows an archaeointensity estimate to be obtained for each magnetic component or heating event. If similar intensities are found for each overprint, and if there is reason to believe that these may have been recorded at more or less the same time as the primary magnetisation, the results could be averaged. If distinct intensities are found, it could instead be possible to estimate each separate heating event, allowing a gauge on the lifespan of the pottery, making it possible to interpret whether the pottery is seen as disposable or whether it is used over an extended period of time. This would also benefit the archaeologists as it would provide more ways to interpret an artefact's lifespan. This approach would require altering the number of temperature steps

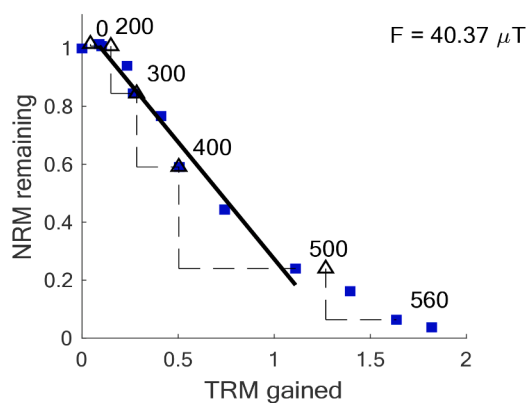
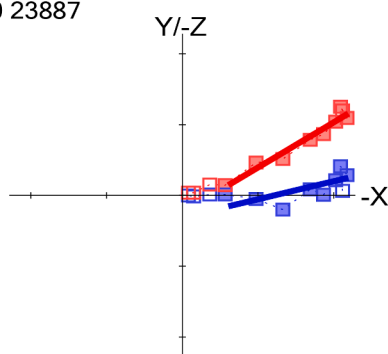
A. 2114 7423



B. 4381 16858



C. 6140 23887



D. 4381 18213

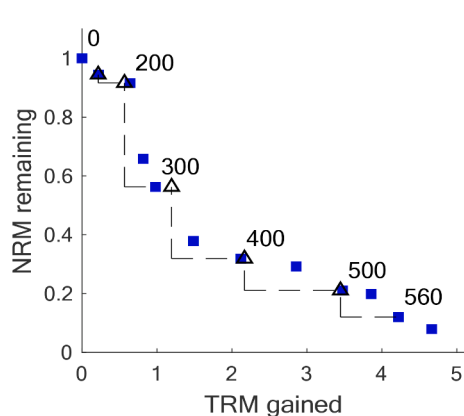
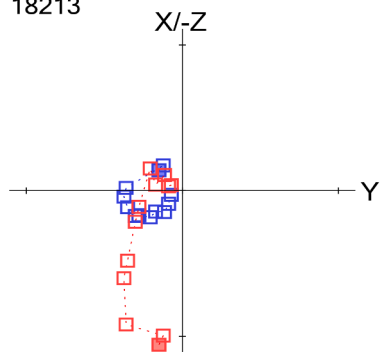


**Fig. 5.** The Zijderveld and Arai plot (NRM remaining versus TRM gained (normalised to the total NRM)) for the three accepted archaeointensity results from samples A. 2114 7423, B. 4381 16,858 and C. 6140 23887. Dashed lines on the Arai plot indicates the pTRM checks back to a previous temperature. The solid black line shows the line of best fit for the accepted portion of the plot. Numbers indicate temperature step in °C. Fig. 5D is an example of a sample that was rejected. Red represents the horizontal plane and blue represents the vertical plane on the Zijderveld plot. (For interpretation of the references to colour in this figure legend, the reader is referred to the web version of this article.)

**Table 1**

The accepted archaeointensity results alongside the dates for the context that the sample was located. The archaeointensity estimates were evaluated using SELCRIT2 criteria (Biggin et al., 2007) on paleointensity.org (Béguin et al., 2020). Standard error of the archaeointensity estimate is given.

Sample	95% Date Range (BCE)	$B_{anc}$ ( $\mu T$ )	n	f	$\beta$	q	$MAD_{anc}$	$\alpha$	$\gamma$	DRAT
2114 7423	3015–2880	$40.3 \pm 2.5$	9	0.847	0.061	11.7	3.8	6.6	3.6	2.6
4381 16,858	2915–2680	$35.6 \pm 1.4$	9	0.838	0.037	19.1	4.0	1.9	3.6	3.0
6140 23,887	3100–2700	$40.4 \pm 2.7$	8	0.741	0.066	9.0	5.6	9.9	2.4	3.8

used in the Thellier experiment as the temperature steps need to be narrower than the steps used here, to ensure that enough data points are available for each overprint to make the archaeointensity result robust.

#### 4.2. Comparison to other datasets

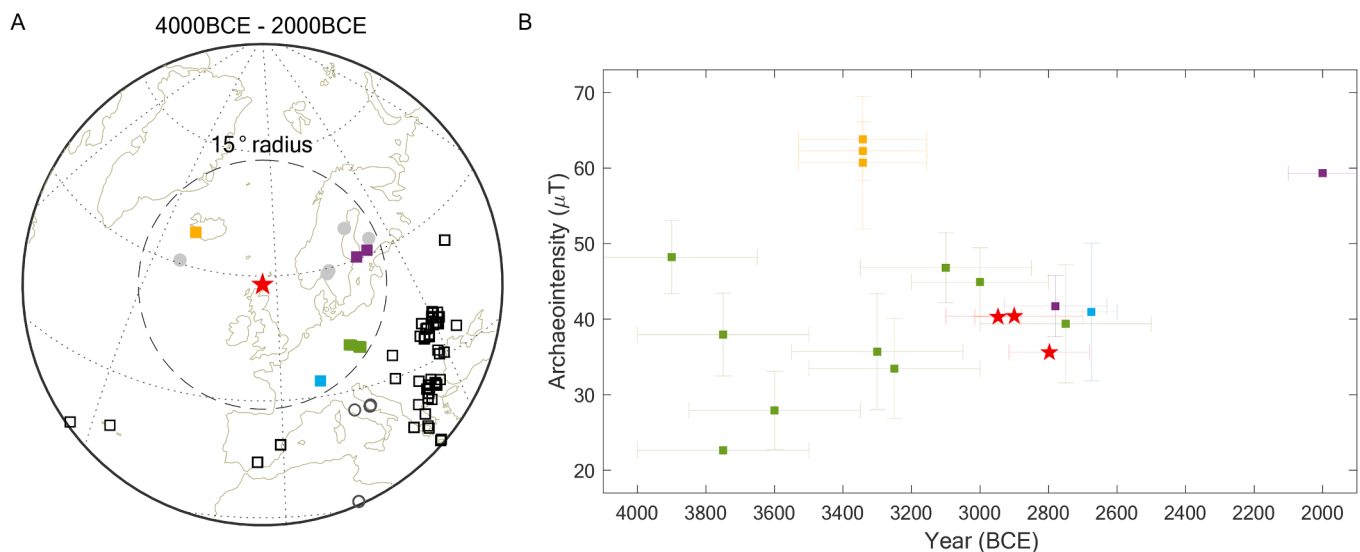
It is usual practice for several archaeointensity results to be obtained from each archaeological deposit or context and an average obtained. Although limited results were obtained in this feasibility study, it is still of interest to compare them to other data from the Neolithic period. To collect previously published Neolithic data an enquiry to the GEOMAGIA50.v3.3 database (Brown et al., 2015) was made for all the intensity data available (from archaeological materials, lavas and sediments) in a  $15^\circ$  radius from the Neolithic period, defined for this purpose as 4000BCE to 2000BCE. In addition to the absolute palaeointensity data from heated materials, available sediment records from the same query parameters with relative palaeointensity data were selected from the collection used to constrain the pfm9k.1a geomagnetic field model (Nilsson et al., 2014); see below for a description of the model. The locations where study results were obtained from the inquiry are shown in Fig. 6.

The sparsity of absolute intensity data in and around the British Neolithic is apparent. Within a  $15^\circ$  radius from the Ness of Brodgar in the Neolithic period (4000–2000BCE) there are archaeointensity estimates from (i) lava flows in Iceland (Schweitzer and Soffel, 1980; Stanton et al., 2011; Tanaka et al., 2012), (ii) three potsherds from two sites in Finland (Pesonen et al., 1995), (iii) five intensity estimates from

burnt earth, kilns and potsherds from five different archaeological sites in the Czech Republic (Bucha, 1967) and (iv) in Switzerland where three sherds provide a site average, with an independent date obtained through radiocarbon and dendrochronology (Kapper et al., 2015). Additionally, there are relative palaeointensities from five lake and marine sediment records (Channell et al., 1997; Ojala and Saarinen, 2002; Snowball and Sandgren, 2002; Zillén, 2003; Snowball et al., 2007).

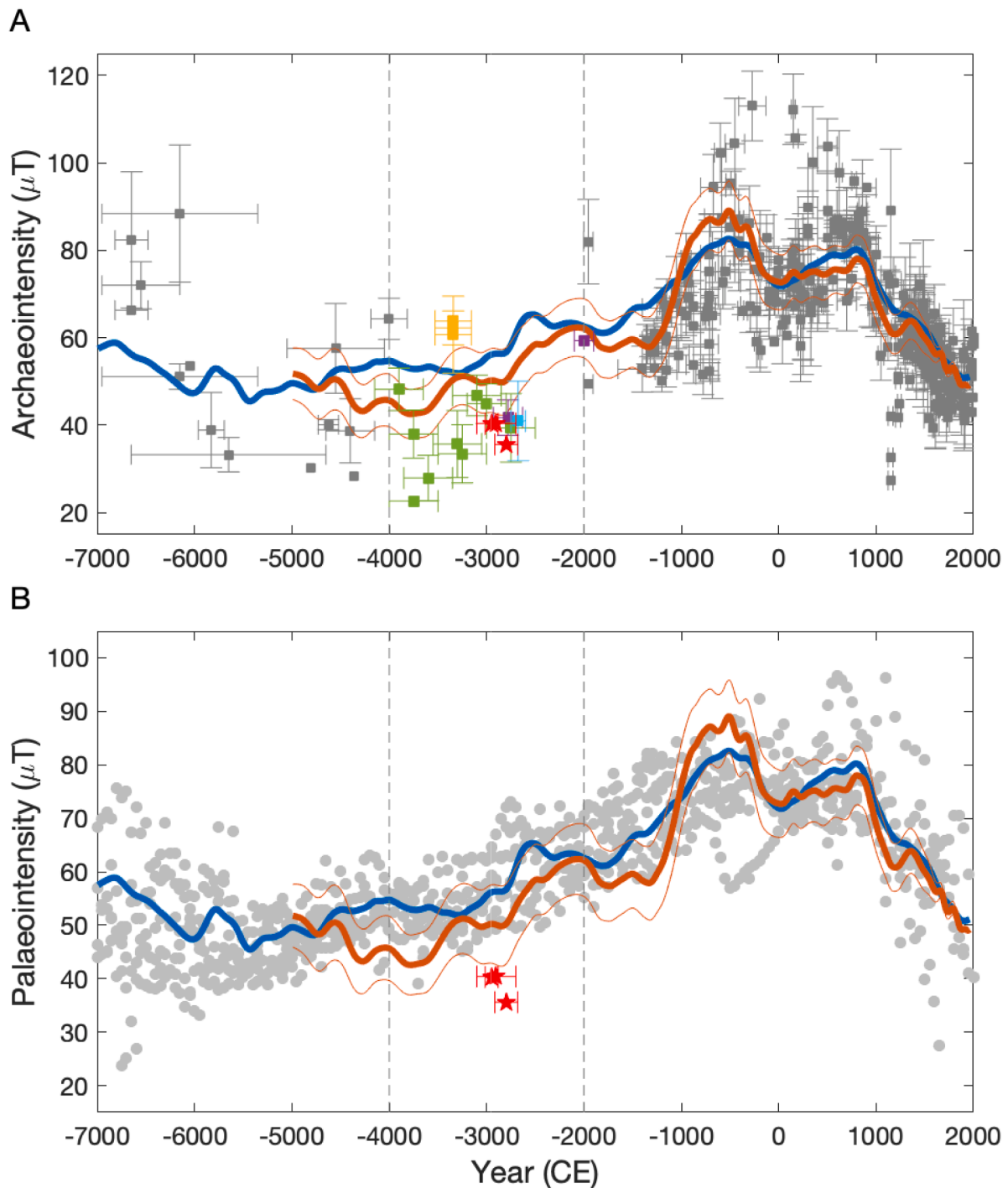
The three archaeointensity results from Ness of Brodgar ( $58.9^\circ$  N,  $3.2^\circ$ W) are plotted in Fig. 6B alongside the relocated (assuming a geocentric axial dipole (GAD) field) published archaeointensity data obtained within a  $15^\circ$  radius. It can be seen that the new results are consistent with the, albeit limited, data of similar age. Obviously the most reliable archaeo- and palaeointensities come from studies that have multiple measurements from the same contexts, so a site average is recorded, as is the case for the Swiss study of Kapper et al. (2015). Of note, is that the Ness of Brodgar data is consistent with this Swiss data point. A significant proportion of other available estimates come from single artefacts (both Finland and the Czech Republic). The archaeointensity results from the Czech Republic are also from an older study (Bucha, 1967) and are derived from an out-dated palaeointensity technique (double-heating method, with no pTRM checks), which means that the reliability is unknown and the dating methods may be outdated. It is therefore not surprising that the Bucha (1967) dataset is somewhat scattered however we note that the younger Bucha data that covers the same age as the Ness of Brodgar results are not noticeably outliers.

Fig. 7A. and B. shows all archaeointensity data and sedimentary



**Fig. 6.** A. A map showing the location of archaeomagnetic and sedimentary samples from Geomag50.v3.3 (Brown et al., 2015) during the Neolithic period 4000–2000BCE and (red star) the location of the Ness of Brodgar. The dotted line shows a  $15^\circ$  (1666 km) radius around the Ness of Brodgar site. Purple squares: archaeomagnetic data from Finland (Pesonen et al., 1995). Yellow square: archaeomagnetic data from Iceland (Stanton et al., 2011; Schweitzer and Soffel, 1980). Green squares: archaeomagnetic data from Czech Republic (Bucha, 1967). Blue square: archaeomagnetic data from Switzerland (Kapper et al., 2015). Grey filled circles: sedimentary data from Sweden (Snowball and Sandgren, 2002; Snowball et al., 2007; Zillén, 2003), from Finland (Snowball et al., 2007; Ojala and Saarinen, 2002) and from the North Atlantic (Channell et al., 1997). Open black squares and circles: archaeomagnetic and sedimentary data from elsewhere in Europe between 4000 and 2000BCE. Fig. 6B. The archaeointensity results (symbol colour and shape as given in Fig. 6A), relocated assuming a GAD field, from the  $15^\circ$  radius Geomag50.v3.3 enquiry spanning the Neolithic period. Intensity errors are  $1\sigma$ . Ness of Brodgar age errors are 95%. Other age errors are those stated in Geomag50.V3.3. (For interpretation of the references to colour in this figure legend, the reader is referred to the web version of this article.)





**Fig. 7.** A. Plot of all archaeointensity results from a  $15^\circ$  radius of the Ness of Brodgar relocated assuming a GAD field, between 7000BCE to 2000CE. The Neolithic period is highlighted by black dotted lines, with the archaeointensity results following the same colour and shape scheme as Fig. 6. All results that fall outside the Neolithic period are shown as grey squares. Red curve: ARCH-UK.1 (Batt et al., 2017). Blue curve: pfmk.1a (Nilsson et al., 2014). Intensity errors are  $1\sigma$ . Ness of Brodgar age errors are 95%. Other age errors are those stated in Geomag50.V3.3, which consist of 72, with unspecified age error, 223 with estimated age error, 79 with 1 standard deviation age error and 6 with 2 standard deviation age error. Fig. 7B. Plot of all sedimentary palaeointensity results within a  $15^\circ$  radius of the study site (grey circles), relocated assuming a GAD field using the intensity scaling according to Nilsson et al. (2014), between 7000BCE to 2000CE. The Neolithic period is highlighted by black dotted lines. The new Ness of Brodgar results are plotted by red stars as comparison. As in Fig. 7A. Red curve: ARCH-UK.1 (Batt et al., 2017). Blue curve: pfmk.1a (Nilsson et al., 2014). (For interpretation of the references to colour in this figure legend, the reader is referred to the web version of this article.)

palaeointensity data respectively, within a  $15^\circ$  radius of the Ness of Brodgar ( $58.9^\circ$  N,  $3.2^\circ$  W) relocated assuming a geocentric axial dipole (GAD) field over the past 9000 years. Relative palaeointensities from the five different sediment records were binned in 50-year time steps and scaled to absolute intensities according to Nilsson et al. (2014). The data are plotted alongside the intensity predictions from two geomagnetic

models, ARCH-UK.1. (Batt et al., 2017) and pfmk.1a (Nilsson et al., 2014). ARCH-UK.1 is an archaeomagnetic field model created specifically for UK magnetic studies, where more weight is placed on UK data (from latitudes  $49^\circ$  N to  $61^\circ$  N and longitudes of  $11^\circ$  W and  $2^\circ$  E) during the modelling process. The pfm9k.1a model is a global geomagnetic reconstruction based on archaeomagnetic and sedimentary data with

optimally adjusted timescales. The sediment data were tuned to a preliminary model prediction to reduce model smoothing resulting from chronologic inconsistencies in the data.

The new Ness of Brodgar data are some of the lowest intensities recorded in the region over the past 9000 years, but fall largely within the  $2\sigma$  uncertainty level of ARCH-UK.1. It is worth noting that our data likely represent an upper estimate as no correction has been made for the likely quicker cooling experienced during the archaeointensity experiment compared to the original manufacturing (Kostadinova-Avramova and Jordanova, 2019). As shown in Fig. 7B, the scatter is generally quite large between contemporaneous archaeointensity data prior to 1000AD and consequently this is also true for the uncertainties in the ARCH-UK.1 model prior to 1000AD.

We note that this period of lower archaeointensity in the Neolithic period is not observed in the sedimentary data; however, the internal consistency between the five archaeological records is quite high. The predicted intensity variations from the pfm9k.1a model, which is heavily constrained by sediment records for this time period, naturally follows the sedimentary data and shows neither the same highs nor the same lows, e.g. during the Neolithic period, as the ARCH-UK model prediction. A potential explanation for this discrepancy between the two datasets, and associated models, is the post-depositional smoothing of the sedimentary data, related to the gradual process by which the magnetic signal is being acquired, or 'locked-in', during burial of the sediments. Mellström et al. (2015) showed how this process could explain both the smoothing and slight temporal offset of two Scandinavian lake sediment records, successfully reconciling the data with archaeomagnetic field model predictions. Incorporating these methods when building geomagnetic field models could, as demonstrated by Nilsson et al. (2018), potentially pave the way for high-resolution archaeomagnetic dating prior to the past 2–3 millennia.

## 5. Conclusion

This research has demonstrated that it is possible to obtain measurements of the intensity of the past geomagnetic field from Neolithic pottery from Ness of Brodgar, despite the fact that the material is low-fired and friable. The three new data points obtained in this investigation fit the general trend of the geomagnetic field behaviour in the Neolithic, although the new Ness of Brodgar data has a tendency towards lower intensity values.

The current generation of geomagnetic field models are either poorly constrained (large uncertainties) prior to the last 2–3 millennia due to lack of archaeomagnetic data or rely on sedimentary data, which may result in excessive smoothing due to post-depositional processes. This highlights the need for more archaeomagnetic investigations, because at present, GEOMAGIA50.v3.3 contains data points from only a small number of countries and at a limited range of latitudes, especially for the earlier archaeological time periods.

This research has identified procedures to reduce unfavourable types of sample behaviour for future archaeointensity research on Neolithic pottery. This should allow behaviours including sample alteration, multi-domain effects and issues with the microwave system to be reduced. These procedures should ensure an improved success rate, which means that there is significant potential for further work, thus providing new and much needed data to improve our understanding of how the geomagnetic field has changed during the Neolithic, and in turn allowing the potential for archaeointensity dating within the UK to be explored.

## Declaration of Competing Interest

We have no conflicts of interest to disclose and we confirm that this is original work and it is not under consideration for publication elsewhere.

## Acknowledgements

We thank Roy Towers of the Ness of Brodgar Project for providing pottery samples. Elliot Hurst is thanked for the aid with sample preparation at the Geomagnetic Laboratory, University of Liverpool. MLA would also like to thank the Andy Jagger Fund, University of Bradford, for supporting the stay at the University of Liverpool and Crafoord Grant, Sweden, No. 20160763. The radiocarbon dates were funded by AHRC NF/2017/2/7. We are grateful for the two thorough reviews of a previous version of this manuscript by anonymous reviewers, and two further anonymous reviewers for the resubmitted manuscript. We would also like to thank the editors of the journal.

## Appendix A. Supplementary data

Supplementary data to this article can be found online at <https://doi.org/10.1016/j.jasrep.2021.102895>.

## References

- Aitken, M.J., Hawley, H.N., Weaver, G.H., 1963. Magnetic dating: further archaeomagnetic measurements in Britain. *Archaeometry* 6 (1), 76–80.
- Atkinson, D., King, J.A., 2005. Fine particle magnetic mineralogy of archaeological ceramics. *J. Phys. Conf. Ser.* 17, 145–149.
- Batt, C.M., Brown, M.C., Clelland, S.-J., Korte, M., Linford, P., Outram, Z., 2017. Advances in archaeomagnetic dating in Britain: new data, new approaches and a new calibration curve. *J. Archaeol. Sci.* 85, 66–82.
- Béguin, A., Paterson, G.A., Biggin, A. J. and de Groot, L. V., 2020. Paleointensity.org: An Online, Open Source, Application for the Interpretation of Paleointensity Data. *Geochemistry, Geophysics, Geosystems* 21 (5), e2019GC008791.
- Ben-Yosef, E., Tauxe, L., Levy, T.E., Shaar, R., Ron, H., Najjar, M., 2009. Geomagnetic intensity spike recorded in high resolution slag deposit in Southern Jordan. *Earth Planet. Sci. Lett.* 287 (3–4), 529–539.
- Biggin, A.J., Paterson, G.A., 2014. A new set of qualitative reliability criteria to aid inferences on palaeomagnetic dipole moment variations through geological time. *Front. Earth Sci.* 2, 24.
- Biggin, A., Perrin, M., Dekkers, M., 2007. A reliable absolute palaeointensity determination obtained from a non-ideal recorder. *Earth Planet. Sci. Lett.* 257 (3–4), 545–563.
- Brown, M. C., Donadini, F., Korte, M., Nilsson, A., Korhonen, K., Lodge, A., Lengyel, S. N. and Constable, C. G., 2015. GEOMAGIA50.v3: 1. general structure and modifications to the archeological and volcanic database. *Earth, Planets and Space* 67(1), 83.
- Bucha, V., 1967. Intensity of the Earth's magnetic field during archaeological times in Czechoslovakia. *Archaeometry* 10 (1), 12–22.
- Calvo-Rathert, M., Morales Contreras, J., Carrancho, Á., Camps, P., Goguitchaichvili, A., Hill, M.J., 2019. Reproducibility of archaeointensity determinations with a multimethod approach on archaeological material reproductions. *Geophys. J. Int.* 218 (3), 1719–1738.
- Card, N., 2012. The Ness of Brodgar. *Br. Archaeol.* 128, 14–21.
- Card, N., 2018. The Ness of Brodgar Uncovering Orkney's Neolithic heart. *Curr. Archaeol.* 335, 20–28.
- Card, N., Mainland, I., Timpany, S., Towers, R., Batt, C., Ramsey, C.B., Dunbar, E., Reimer, P., Bayliss, A., Marshall, P., Whittle, A., 2017. To cut a long story short: formal chronological modelling for the late Neolithic Site of Ness of Brodgar, Orkney. *Eur. J. Archaeol.* 21 (2), 217–263.
- Casas, L., Shaw, J., Gich, M., Share, J.A., 2005. High-quality microwave archaeointensity determinations from an early 18th century ad English brick kiln. *Geophys. J. Int.* 161 (3), 653–661.
- Channell, J.E.T., Hodell, D.A., Lehman, B., 1997. Relative geomagnetic paleointensity and  $\delta 180$  at ODP Site 983 (Gardar Drift, North Atlantic) since 350 ka. *Earth Planet. Sci. Lett.* 153 (1–2), 103–118.
- Clark, A.J., Tarling, D.H., Noël, M., 1988. Developments in archaeomagnetic dating in Britain. *J. Archaeol. Sci.* 15 (6), 645–667.
- Cowie, T., MacSween, A., 1999 Grooved Ware from Scotland: a review. in: Cleal, R. M., A. (ed.) *Grooved Ware in Britain and Ireland. Vol. Neolithic Studies Group Seminar Papers 3*. Oxford: Oxbow Books.
- Day, R., Fuller, M., Schmidt, V.A., 1977. Hysteresis properties of titanomagnetites: grain-size and compositional dependence. *Phys. Earth Planet. Inter.* 13 (4), 260–267.
- Dunlop, D.J., Özdemir, Ö., 1997. *Rock Magnetism: Fundamentals and Frontiers*. Cambridge University Press, Cambridge.
- Dunlop, D. J., 2002. Theory and application of the Day plot (Mrs/Ms versus Hcr/Hc) 1. Theoretical curves and tests using titanomagnetite data. *Journal of Geophysical Research: Solid Earth* 107(B3), EPM 4-1-EPM 4-22.
- Forum on Information Standards in Heritage, 2016. Chronological guide for recording sites and monuments [Medium]. Place Published: <http://heritage-standards.org.uk/chronology/> Updated Last Update Date.
- Genevey, A., Gallet, Y., Thébault, E., Jesset, S., Le Goff, M., 2013. Geomagnetic field intensity variations in Western Europe over the past 1100 years. *Geochem. Geophys. Geosyst.* 14 (8), 2858–2872.

- Hervé, G., Chauvin, A., Lanos, P., 2013. Geomagnetic field variations in Western Europe from 1500BC to 200AD. Part II: new intensity secular variation curve. *Phys. Earth Planet. Inter.* 218, 51–65.
- Hill, M.J., Gratton, M.N., Shaw, J., 2002. A comparison of thermal and microwave palaeomagnetic techniques using lava containing laboratory induced remanence. *Geophys. J. Int.* 151 (1), 157–163.
- Hill, M.J., Shaw, J., 1999. Palaeointensity results for historic lavas from Mt Etna using microwave demagnetization/remagnetization in a modified Thellier-type experiment. *Geophys. J. Int.* 139 (2), 583–590.
- Jonkers, A.R.T., Jackson, A., Murray, A., 2003. Four centuries of geomagnetic data from historical records. *Rev. Geophys.* 41 (2).
- Kapper, K.L., Donadini, F., Hirt, A.M., 2015. Holocene archeointensities from mid European ceramics, slags, burned sediments and cherts. *Phys. Earth Planet. Inter.* 241, 21–36.
- Kostadinova-Avramova, M., Jordanova, N., 2019. Study of cooling rate effect on baked clay materials and its importance for archaeointensity determinations. *Phys. Earth Planet. Inter.* 288, 9–25.
- Kovacheva, M., 1997. Archaeomagnetic database from Bulgaria: the last 8000 years. *Phys. Earth Planet. Inter.* 102 (3–4), 145–151.
- Kovacheva, M., Boyadziev, Y., Kostadinova-Avramova, M., Jordanova, N., Donadini, F., 2009. Updated archeomagnetic data set of the past 8 millennia from the Sofia laboratory, Bulgaria. *Geochem. Geophys. Geosyst.* 10 (5).
- Leonhardt, R., 2006. Analyzing rock magnetic measurements: the RockMagAnalyzer 1.0 software. *Comput. Geosci.* 32 (9), 1420–1431.
- Malin, S. C. R., Bullard, E. and Munk, W. H., 1981. The direction of the Earth's magnetic field at London, 1570-1975. *Philosophical Transactions of the Royal Society of London. Series A, Mathematical and Physical Sciences* 299 (1450), 357-423.
- Mellström, A., Nilsson, A., Stanton, T., Muscheler, R., Snowball, I., Suttie, N., 2015. Post-depositional remanent magnetization lock-in depth in precisely dated varved sediments assessed by archaeomagnetic field models. *Earth Planet. Sci. Lett.* 410, 186–196.
- Nilsson, A., Holme, R., Korte, M., Suttie, N., Hill, M., 2014. Reconstructing Holocene geomagnetic field variation: new methods, models and implications. *Geophys. J. Int.* 198 (1), 229–248.
- Nilsson, A., Suttie, N., Hill, M.J., 2018. Short-term magnetic field variations from the post-depositional Remanence of Lake Sediments. *Front. Earth Sci.* 6 (39).
- Ojala, A.E.K., Saarinen, T., 2002. Palaeosecular variation of the Earth's magnetic field during the last 10000 years based on the annually laminated sediment of Lake Nautajarvi, central Finland. *Holocene* 12 (4), 391–400.
- Paterson, G.A., Tauxe, L., Biggin, A.J., Shaar, R., Jonestrask, L.C., 2014. On improving the selection of Thellier-type paleointensity data. *Geochem. Geophys. Geosyst.* 15 (4), 1180–1192.
- Pesonen, L.J., Leino, M.A.H., Nevanlinna, H., 1995. Archaeomagnetic Intensity in Finland during the Last 6400 Years: evidence for a Latitude-Dependent Nondipole Field at AD 500. *J. Geomagn. Geoelec.* 47 (1), 19–40.
- Reimer, P.J., Bard, E., Bayliss, A., Beck, J.W., Blackwell, P.G., Ramsey, C.B., Buck, C.E., Cheng, H., Edwards, R.L., Friedrich, M., Grootes, P.M., Guilderson, T.P., Hafliðason, H., Hajdas, L., Hatté, C., Heaton, T.J., Hoffmann, D.L., Hogg, A.G., Hughen, K.A., Kaiser, K.F., Kromer, B., Manning, S.W., Niu, M.u., Reimer, R.W., Richards, D.A., Scott, E.M., Southon, J.R., Staff, R.A., Turney, C.S.M., van der Plicht, J., 2013. IntCal13 and Marine13 Radiocarbon Age Calibration Curves 0–50,000 Years cal BP. *Radiocarbon* 55 (4), 1869–1887.
- Roberts, A.P., Tauxe, L., Heslop, D., Zhao, X., Jiang, Z., 2018. A critical appraisal of the “Day” diagram. *J. Geophys. Res. Solid Earth* 123 (4), 2618–2644.
- Schweitzer, C., Soffel, C.H., 1980. Palaeointensity measurements on postglacial lavas from Iceland. *J. Geophys.* 47, 57–60.
- Shaar, R., Ben-Yosef, E., Ron, H., Tauxe, L., Agnon, A., Kessel, R., 2011. Geomagnetic field intensity: how high can it get? How fast can it change? Constraints from Iron Age copper slag. *Earth Planet. Sci. Lett.* 301 (1–2), 297–306.
- Snowball, I., Sandgren, P., 2002. Geomagnetic field variations in northern Sweden during the Holocene quantified from varved lake sediments and their implications for cosmogenic nuclide production rates. *Holocene* 12 (5), 517–530.
- Snowball, I., Zillén, L., Ojala, A., Saarinen, T., Sandgren, P., 2007. FENNOSTACK and FENNORPIS: varve dated Holocene palaeomagnetic secular variation and relative palaeointensity stacks for Fennoscandia. *Earth Planet. Sci. Lett.* 255 (1–2), 106–116.
- Stanton, T., Riisager, P., Knudsen, M.F., Thordarson, T., 2011. New palaeointensity data from Holocene Icelandic lavas. *Phys. Earth Planet. Inter.* 186 (1–2), 1–10.
- Stark, F., Cassidy, J., Hill, M.J., Shaw, J., Sheppard, P., 2010. Establishing a first archaeointensity record for the SW Pacific. *Earth Planet. Sci. Lett.* 298 (1–2), 113–124.
- Stillinger, M.D., Feinberg, J.M., Frahm, E., 2015. Refining the archaeomagnetic dating curve for the Near East: new intensity data from Bronze Age ceramics at Tell Mozan, Syria. *J. Archaeol. Sci.* 53, 345–355.
- Tanaka, H., Hashimoto, Y., Morita, N., 2012. Palaeointensity determinations from historical and Holocene basalt lavas in Iceland. *Geophys. J. Int.* 189 (2), 833–845.
- Thellier, E., Thellier, O., 1959. Sur l'intensité du champ magnétique terrestre dans le passé historique et géologique. *Annales de Geophysique* 15, 285.
- Walton, D., Share, J., Rolph, T.C., Shaw, J., 1993. Microwave magnetisation. *Geophys. Res. Lett.* 20 (2), 109–111.
- Whittle, A., 2017. *The Times of their Lives: Hunting History in the Archaeology of Neolithic Europe*. Oxbow Books.
- Yu, Y., Dunlop, D.J., 2002. Multivectorial paleointensity determination from the Cordova Gabbro, southern Ontario. *Earth and Planetary Science Letters* 203 (3–4), 983–998. [https://doi.org/10.1016/S0012-821X\(02\)00900-7](https://doi.org/10.1016/S0012-821X(02)00900-7). ISSN 0012-821X.
- Yu, Y., Tauxe, L., Genevey, A., 2004. Toward an optimal geomagnetic field intensity determination technique. *Geochem. Geophys. Geosyst.* 5 (2).
- Zananiri, I., Batt, C.M., Lanos, P.h., Tarling, D.H., Linford, P., 2007. Archaeomagnetic secular variation in the UK during the past 4000 years and its application to archaeomagnetic dating. *Phys. Earth Planet. Inter.* 160 (2), 97–107.
- Zillén, L., 2003. *Setting the Holocene Clock Using Varved Lake Sediments*. Lund University, Lund.